

EFFECT OF MICROSTRUCTURES ON LCF-BEHAVIOUR OF STEELS IN HIGH PRESSURE HYDROGEN ENVIRONMENT

K.-T. Rie and W. Kohler \*

Low-cycle fatigue behaviour of low-alloyed and high-alloyed steels has been investigated in air as well as in hydrogen environment. Various heat treatment conditions were included in this study.

It has been found that the hydrogen environment can drastically decrease the fatigue life in LCF-regime. The fatigue life can be represented by an analogous equation to Coffin-Manson relation. The fatigue crack growth rates are determined. Fracture mechanics approach has revealed that a close correlation exists between the crack growth rate and the commonly employed LCF-data. The roll of the microstructure in hydrogen-assisted cracking has been shown.

INTRODUCTION

Low-cycle fatigue (LCF) is an urgent problem in current engineering application, for example, pressure vessels, gas turbines and nuclear reactors. It is known that environment can seriously degrade the mechanical properties of the many of the commonly used steels (1).

The purpose of this work is to establish a correlation between fatigue life in LCF-regime and high pressure hydrogen environment. The effect of various microstructures on LCF-behaviour is included in the study. Fracture mechanical aspects of crack growth rate in LCF-regime is related to conventional LCF-data.

EXPERIMENTAL PROCEDURE

Tests were conducted in strain-controlled tension-compression. Both smooth and notched cylindrical specimens were used.

The conventional LCF-data were obtained by means of hysteresis curves, cyclic strain-hardening/softening curve and cyclic stress-strain curve, while the potential drop method was adopted to achieve data for the crack growth rate.

The failure criterion used is the critical number of cycles  $N_{cr}$  which is defined as the onset of rapid tensile load drop and is comparable with that recommended in § 8.9.2 of ASTM Standard E 606-77 T.

\* Institut für Schweißtechnik und Werkstofftechnologie, TU Braunschweig

TABLE 1 - Properties of heat treated Steels

Steel	Heat Treatment Condition	Mechanical Properties			
		yield strength	ultimate strength	reduction of area	elongation
StE 460	normalized martensitic	510 N/mm <sup>2</sup>	680 N/mm <sup>2</sup>	68 %	28 %
		800 N/mm <sup>2</sup>	975 N/mm <sup>2</sup>	55 %	15 %
X8 CrNiMo VNb 1613	annealed annealed and aged	300 N/mm <sup>2</sup>	625 N/mm <sup>2</sup>	66 %	49 %
		325 N/mm <sup>2</sup>	630 N/mm <sup>2</sup>	65 %	46 %

The test materials were low-alloyed ferritic steel StE 460 and austenitic steel X8 CrNiMoVNb 1613. In order to investigate the effect of microstructures two different heat treatments are chosen for both steels. The mechanical properties and heat treatment conditions are shown in Table 1.

RESULTS AND DISCUSSION

Conventional LCF-Data

It has been reported (2) that the fatigue life in LCF-regime can be well described by the analogous equation to Coffin-Manson relation using the critical number of cycles  $N_{cr}$  instead of the number of cycles to failure  $N_f$ :

$$N_{cr}^{\alpha} \cdot \Delta \epsilon_{pl} = C \quad (1)$$

Previous work (3-4) has shown that even for various environments the fatigue life can be expressed by eq. (1). The experimental results obtained with smooth and notched specimens of the steels StE 460 and X8 CrNiMoVNb 1613 in air and under high pressure hydrogen are shown in Fig. 1.

Fig. 1a shows the fatigue life curves of StE 460 notched specimens in both martensitic and nomalized conditions after testing in air and high pressure hydrogen. It can be seen that the fatigue life of the material tested in hydrogen environment is drastically reduced compared with that in air. In hydrogen environment the microstructure has evidently a remarkable effect on low-cycle fatigue endurance, while the fatigue life was not influenced by microstructure when tested in air. It should be mentioned that the steel StE 460 shows a different ductility depending on the heat treatment conditions. In hydrogen environment the coarse lamellar martensitic microstructure was more susceptible to hydrogen attack.

As expected, the fatigue life of X8 CrNiMoVNb 1613 was influenced by hydrogen environment not so significantly. Fig. 1b indicates that the effect of microstructure on fatigue life for X8 CrNiMoVNb 1613 is practically negligible irrespective of the environment.

For design of structures subject to cyclic straining the cyclic stress-strain curve is essential to characterize the cyclic behaviour of materials (5). By plotting  $\Delta \sigma_{cr}^{\alpha}$  at  $N_{cr}/2$  versus corresponding  $\Delta \epsilon_a$  the cyclic crack

stress-strain curve is obtained, while  $\Delta\sigma$  at  $N_f/2$  is chosen to determine the conventional cyclic stress-strain curve. Fig. 2 shows the cyclic crack stress-strain curve of normalized StE 460 tested in air and hydrogen environment. The normalized specimen is characterized by considerable cyclic strain-hardening. The following relation has been obtained:

$$\Delta\sigma_{Cr}^{**}/2 = K' (\Delta\varepsilon_{p1}/2)^{n'} \quad (2)$$

with  $K' = 1700 \text{ N/mm}^2$ ,  $n' = 0,238$  in air

and  $K' = 1400 \text{ N/mm}^2$ ,  $n' = 0,205$  in hydrogen

Fracture Mechanical Aspects

The stress intensity factor  $\Delta K$ , is widely used for correlation of fatigue crack growth rate. As the stress intensity concept is based on linear elastic analysis, its validity is consequently restricted to situations where the plastic zone size is small compared to the other geometrical dimensions.

From Fig. 3 it is evident that there exists a correlation between cyclic flow behaviour and crack growth rate. For LCF-regime Boettner, Laird and McEvily (6) adopted an approach which is fundamentally similar in concept to the stress intensity factor  $\Delta K$ . They defined a strain intensity factor

$$\Delta K_{\varepsilon} = \Delta\varepsilon_a \cdot \sqrt{a} \quad (3)$$

and obtained

$$da/dN = A \cdot (\Delta\varepsilon_a \sqrt{a})^n \quad (4)$$

In LCF-regime it has been shown that fatigue crack propagation in stage II mode occupies most of the life time. Inserting  $n = 2$  in eq. (4) and integrating between appropriate values of  $a$

$$\Delta\varepsilon_a^2 \cdot N_{II} = k \cdot \ln(a_f/a_0) \quad (5)$$

and eq. (5) reduces to eq. (1), Coffin-Manson relation, if  $a_0$  and  $a_f$  are approximately the same for all conditions. This indicates that Coffin-Manson relation can be understood as a crack growth law.

Results of the crack growth measurement for normalized StE 460 are plotted in Fig. 4 in terms of a strain intensity factor  $\Delta K_{\varepsilon}$ . The value of the exponent  $n$  was determined from the plot shown in Fig. 4.  $n$  is about 2,0 - 2,2 for both air and hydrogen environment. It can be seen that the crack growth rate in hydrogen environment is considerably higher than in air.

Being based on linear elastic analysis  $\Delta K$ - and  $\Delta K_{\varepsilon}$ -values have no physical meaning for low-cycle fatigue involving large scale plasticity. Thus, a more general parameter is needed which can account for large plasticity effects.

Based on the crack tip strain field interpretation J-integral has been successfully employed in recent years as a criterion for static plastic fracture (7-8).

Kaisand and Mowbray (9) have proposed recently a model to describe crack growth rate in LCF-regime which involves a J-integral analysis and a crack growth hypothesis in terms of  $\Delta J$  developed by Dowling and Begley (10). A re-

relationship for half-circular surface crack is derived that has strain energy density as the controlling variable:

$$\Delta J = \Delta J_{e1} + \Delta J_{p1} \quad (6)$$

$$\Delta J = 3,2 \cdot \Delta W_{e1} \cdot a + 5 \cdot \Delta W_{p1} \cdot a \quad (7)$$

The plastic strain energy density  $\Delta W_{p1}$  can be estimated approximately from stress-strain hysteresis loops (11-12).

In Fig. 5 the fatigue crack growth rate  $da/dN$  versus cyclic  $\Delta J$ -data is shown for tests in air and hydrogen environment. It is found that the data can be represented by a relationship of the form

$$da/dN = A \cdot (\Delta J)^m \quad (8)$$

The material constant  $m$  has a value of about 1,5 - 1,8 and this is in good agreement with that of Dowling et al (11-13). Their  $m$ -value is about 1,7 independent of the specimen geometries.

Recently Kaisand et al (9) have derived a relationship between the material properties commonly employed to describe low-cycle fatigue and fatigue crack growth rate. With this equation the fatigue crack growth rate curves can be predicted from standard low-cycle fatigue properties. Using the material constants  $\alpha$ ,  $C$ ,  $n'$  and  $K'$  from eqs. (1) and (2) the fatigue crack growth rate  $da/dN$  and  $\Delta J$  are calculated. The comparison of prediction versus experiment has shown that the agreement is quite satisfactory.

#### Microstructural Aspects

Microstructural and fractographic investigations were carried out to analyse the effect of microstructure on LCF-behaviour in hydrogen environment.

It has been found that the quenched martensitic structure is more sensitive to hydrogen-assisted fracture than the tempered bainite or ferrite (14). Fig. 6 indicates that hydrogen diffusion along the prior-austenite grain boundaries as well as along fresh martensite lamellars has caused the decrease in the cohesive strength of the lattice and resulted in the hydrogen-assisted fatigue life reduction.

The fracture mode of the martensitic specimens StE 460 after testing in hydrogen environment was characteristic quasi-cleavage and intergranular cracking (Fig. 7), while ductile striations were found only in specimens tested in air.

In Fig. 8 it can be seen that in specimens of X8 CrNiMoVNb 1613 secondary cracks are formed ahead of the main fatigue crack when tested in hydrogen environment. This suggests that the dissociated hydrogen atoms are segregated at the precipitations of the austenitic steel. This leads to the lowering of the fracture strength by weakening the interface bond. Gerberich et al (15) showed that the hydrogen atoms diffuse from the crack tip into the region of highest stress conditions within the plastic zone. The estimated critical depth of the hydrogen segregation is between 4 - 20  $\mu\text{m}$ . SEM findings indicates the importance of the precipitations as traps and the roll of the stress gradient ahead of the crack tip for hydrogen embrittlement.

CONCLUSIONS

The results obtained in this study can be summerized as follows:

1. The fatigue life in LCF-regime can be represented even for hydrogen environment by an analogous equation to Coffin-Manson relationship.
2. The hydrogen environment can increase the crack growth rate in LCF-regime resulting in a drastical decrease of the fatigue life.
3. Fracture mechanics approach has revealed that the commonly employed LCF-data can be related to the fatigue crack growth rate.
4. The degradation of the fatigue life in hydrogen environment depends strongly on the microstructure of the tested material.

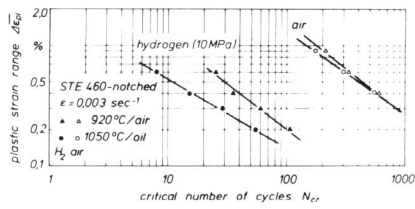
SYMBOLS USED

- $N_{cr}$  = critical number of cycles  
 $\Delta\epsilon_{pl}$  = plastic strain range  
 $\Delta\epsilon_a$  = total strain range  
 $\alpha, C$  = constants  
 $K'$  = cyclic strength coefficient ( $N/mm^2$ )  
 $n'$  = cyclic strain-hardening exponent  
 $\Delta\sigma_{cr}^{**}$  = critical stress range ( $N/mm^2$ )  
 $da/dN$  = crack growth rate (mm/cyc.)  
 $a$  = crack length (mm)  
 $\Delta K$  = stress intensity factor ( $N/mm^{2/3}$ )  
 $\Delta K_E$  = strain intensity factor ( $mm^{1/2}$ )  
 $\Delta J$  = cyclic J-integral ( $mmN/mm^2$ )  
 $\dot{\epsilon}$  = strain rate ( $sec^{-1}$ )  
 $\Delta W$  = range of strain energy density ( $N/mm^2$ )

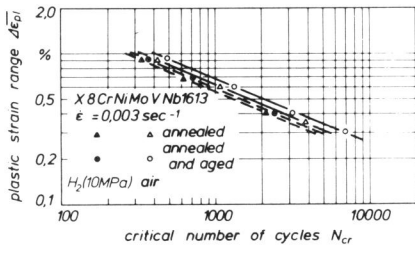
REFERENCES

1. Jewett, R.P., Walter, R.J., Chandler, W.T., and Frohberg, R.P., 1973, NASA-Report, CR-2163.
2. Rie, K.-T., and Stüwe, H.P., 1973, Z. f. Metallkunde, 64, 37.
3. Rie, K.-T., Ruge, J., and Kohler, W., 1979, Proc. JIMIS-2 "Hydrogen in Metals", Minakami Spa, Japan, 629.

4. Lachmann, E., and Rie, K.-T., 1982, to be published in Corrosion Sci.
5. Landgraf, R.W., 1979, Proc. Int. Symp. "Low-cycle Fatigue Strength and Elasto-plastic Behaviour of Materials", DVM, Stuttgart, Germany, 285.
6. Boettner, R.C., Laird, C., and McEvily, A.J., 1965, Trans. AIME, 233, 387.
7. Landes, J.D., and Begley, J.A., 1972, ASTM STP 514, 24.
8. Logsdon, W.A., 1976, ASTM STP 590, 43.
9. Kaisand, L.R., and Mowbray, D.F., 1979, JTEVA 7, 270.
10. Dowling, N.E., and Begley, J.A., 1976, ASTM STP 590, 82.
11. Dowling, N.E., 1976, ASTM STP 601, 19.
12. Dowling, N.E., 1977, ASTM STP 637, 97.
13. Usami, S., Kimoto, H., Enomoto, K., and Shida, S., 1979, Fat.Eng. Mat. Struc., 1, 509.
14. AsaoKa, T., 1979, Proc. JIMIS-2 "Hydrogen in Metals", Minakami Spa, Japan, 161.
15. Gerberich, W.W., Chen, Y.T., and St. John, C., 1975, Met. Trans., 6A, 1485.



a.



b.

Figure 1 Fatigue life curves

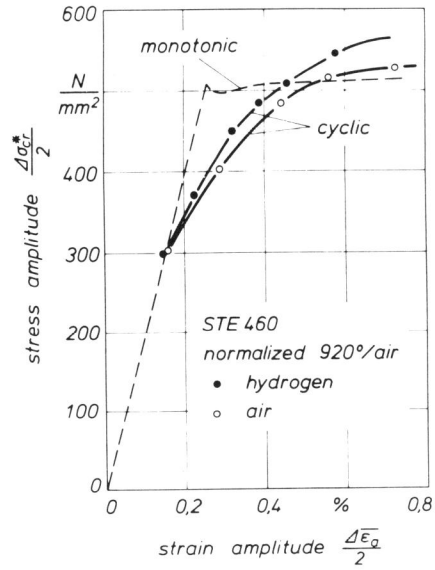


Figure 2 Cyclic crack stress-strain curve

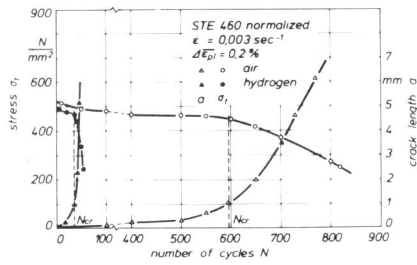


Figure 3 Cyclic flow curve and crack propagation

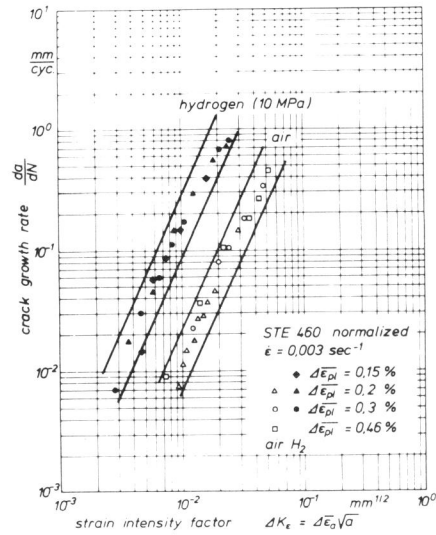


Figure 4 Crack growth rate versus strain intensity factor  $\Delta K_\epsilon$

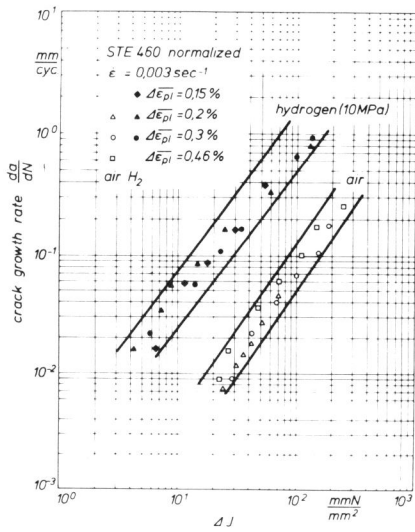


Figure 5 Crack growth rate versus cyclic J-integral ( $\Delta J$ )

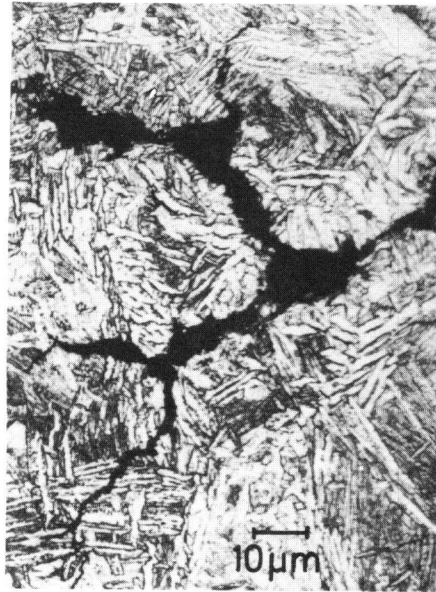


Figure 6 Fatigue crack along prior-austenite grain boundaries

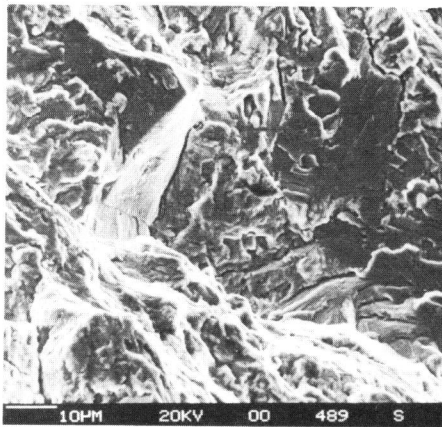


Figure 7 Fracture surface of StE 460 tested in hydrogen environment

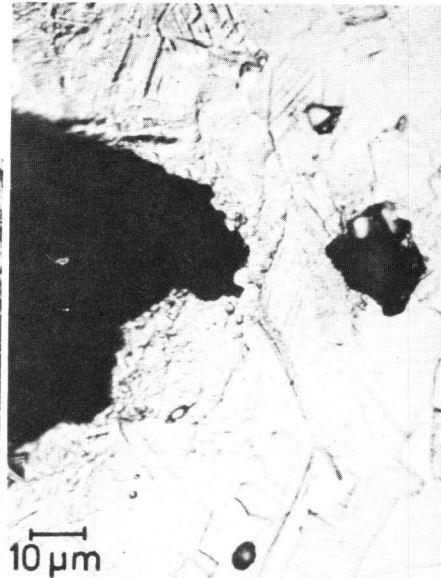


Figure 8 Fatigue crack in hydrogen environment (X8 CrNiMoVNb 1613)